

Performance of quantum heat engines via adiabatic deformation of potential

Kai Li¹, Yang Xiao¹, Jizhou He¹, and Jianhui Wang^{1,2*}

¹Department of Physics, Nanchang University, Nanchang 330031, China

²State Key Laboratory of Surface Physics and Department of Physics, Fudan University, Shanghai 200433, China

(Dated: February 15, 2022)

We present a quantum Otto engine model consisting of two isochoric and two adiabatic strokes, where the adiabatic expansion or compression is realized by adiabatically changing the shape of the potential. Here we show that such an adiabatic deformation may alter operation mode and enhance machine performance by increasing output work and efficiency, even with the advantage of decreasing work fluctuations. If the heat engine operates under maximal power by optimizing the control parameter, the efficiency shows certain universal behavior, $\eta^* = \eta_C/2 + \eta_C^2/8 + O(\eta_C^3)$.

PACS number(s): 05.70.Ln

I. INTRODUCTION

Heat engines should ideally have good performance in finite time [1–6], and operate stably [7–10] by exhibiting small fluctuations. Quantum heat engines [11–27] were observed to operate with novel performance beyond their classical counterparts. These devices with a limited number of freedoms are exposed to not only thermal fluctuations, but also quantum fluctuations related to discrete energy spectra [28–32]. Both fluctuation mechanisms question stable operation of the quantum heat engines [28, 30, 31]. Thermal design and optimization of quantum heat engines [33–35] are therefore expected to consider in order to both the good performance and the stability.

To describe the machine performance, there are usually two benchmark parameters [2, 8, 17, 27, 30]: the thermodynamic efficiency $\eta = \langle w \rangle / \langle q_h \rangle$, where $\langle w \rangle$ is the average work output per cycle and $\langle q_h \rangle$ is the average heat released from the hot reservoir, and the power $\mathcal{P} = \langle w \rangle / \tau_{cyc}$, with the cycle period τ_{cyc} . Ideally, both these two quantities should have large values for excellent performance, but there are always power-efficiency trade-off dilemma [36–41]. An important issue is hence that optimizing the heat engines by determining their efficiency under maximal power [1, 2, 7, 11, 20].

Discreteness of energy levels due to quantization may significantly improve the performance of a quasi-static quantum Otto cycle [19, 29, 30, 42–44] when inhomogeneous shift of energy levels occurs along an isentropic, adiabatic stroke [44, 45]. But the question of how such a shift (due to adiabatic deformation of potential) affects the quantum heat engine in finite-time cycle period, as also hinted in [44], was not answered before. Moreover, the random transitions between discrete energy levels are responsible for quantum fluctuations which dominate at enough low temperatures. A question naturally arises: what is influence of such adiabatic deformation of potential related to discrete energy spectra on the relative

fluctuations that measure the engine stability? As we will demonstrate, the machine efficiency can be improved via control the shape of the potential, without sacrifice of the machine stability.

In this paper, we study a quantum version of Otto engine model which consists of an ideal gas confined in two different potentials. We show that adiabatic shape deformation of the potential can improve work extraction and efficiency, and operates as a heat engine in regions where the engine works as a heater or a refrigerator observed in the absence of the potential deformation. However, for the heat engine working in these extended regions, the efficiency at maximum power shows the universal behavior: $\eta^* = \eta_C/2 + \eta_C^2/8 + O(\eta_C^3)$, with the Carnot efficiency η_C .

II. QUANTUM HEAT ENGINE

We consider an ideal gas of N particles confined in a d -dimensional power-law trap. The system Hamiltonian can be given by

$$\hat{H} = \sum_{\mathbf{i}} \varepsilon_{\mathbf{i}} \hat{a}_{\mathbf{i}}^\dagger \hat{a}_{\mathbf{i}}, \quad (1)$$

where $\varepsilon_{\mathbf{i}} = \langle \mathbf{i} | \hat{H} | \mathbf{i} \rangle$ is the single-particle energy spectrum, and $\hat{a}_{\mathbf{i}}^\dagger$ ($\hat{a}_{\mathbf{i}}$) is the creation (annihilation) operator, with $\mathbf{i} = i_1, \dots, i_d$. Introducing $\hat{G} = \hat{H}/\omega$, the energy spectrum can be written as ($\hbar \equiv 1$): $\varepsilon_{\mathbf{i}} = \omega \langle \mathbf{i} | \hat{G} | \mathbf{i} \rangle = \omega \mathbf{i}^\sigma$, where ω is the energy gap between the ground state and the first-excited state, and $\sigma (> 0)$ depends on the shape of external potential [46]. We call ω the trap frequency and σ the potential exponent. For instance, in a three-dimensional harmonic trap $\varepsilon_{\mathbf{i}} = \omega(i_1 + i_2 + i_3)$ and in a box trap $\varepsilon_{\mathbf{i}} = \omega(i_1^2 + i_2^2 + i_3^2)$, with positive integers $i_{1,2,3}$.

A state of the system at thermal equilibrium with a heat bath of inverse temperature β can be described by the canonical form $\hat{\rho} = \sum_n p_n |n\rangle \langle n| = Z^{-1} \exp(-\beta \hat{H})$, where $p_n = e^{-\beta \varepsilon_n} / Z$ is the probability of finding the system in state $|n\rangle$, with the partition function $Z = \text{Tr}(e^{-\beta \hat{H}})$. The expectation value of \hat{G} for the trapped gas reads $g \equiv \langle \hat{G} \rangle = \text{Tr}(\hat{\rho} \hat{G})$. As a σ -dependent function

*Electronic address: wangjianhui@ncu.edu.cn

g can be expressed as $g = g(\beta\omega, \sigma)$. The internal energy of the system takes the form: $U = \omega g$.

The quantum Otto engine model based on an ideal gas which is confined in two different forms of trapping potential is sketched in Fig. 1(a). It consists of two isochoric processes $A \rightarrow B$ and $C \rightarrow D$, where the gas is weakly coupled to the hot and cold heat reservoirs of constant inverse temperatures β_h^r and $\beta_c^r (> \beta_h^r)$, respectively, and two adiabatic processes $B \rightarrow C$ and $D \rightarrow A$, where the trap exponent (frequency) is changing from σ_h (ω_h) to σ_c [$\omega_c (< \omega_h)$]. The system is allowed to be coupled with the hot (cold) thermal bath in time duration τ_h (τ_c), and it would relax to the thermal state at the ending instant B (D) of the hot (cold) if $\tau_h \rightarrow \infty$ ($\tau_c \rightarrow \infty$). The von Neumann entropy of the system is constant along the adiabatic stroke in which the system evolution is unitary. The time period required for completing the adiabatic expansion (compression) is represented by τ_{hc} (τ_{ch}).

The system entropy reads $S = -\text{Tr}(\hat{\rho} \ln \hat{\rho})$, where $\hat{\rho} = \hat{\rho}(\beta\omega, \sigma)$, and thus the entropy takes the form of $S = S(\beta\omega, \sigma)$. For the gas in a given trap, the entropy S merely depends on the parameter $\beta\omega$: $S = S(\beta\omega)$, and in an adiabatic process $\beta\omega = \text{const}$. However, an adiabatic deformation of trap by changing σ leads to change in the parameter ' $\beta\omega$ ' [44, 45] to keep both particle number N and entropy S constant. Without loss of generality, the relation between the dimensionless internal energies of the system at the four instants of the cycle can be expressed as

$$\begin{aligned} \frac{g_C}{g_B} &= \xi_{hc}(\sigma_c, \sigma_h, \beta_C \omega_c, \beta_B \omega_h), \\ \frac{g_A}{g_D} &= \xi_{ch}(\sigma_c, \sigma_h, \beta_D \omega_c, \beta_A \omega_h). \end{aligned} \quad (2)$$

In the absence of adiabatic potential deformation ($\sigma_c = \sigma_h$), $\beta_C \omega_c = \beta_B \omega_h$ and $\beta_A \omega_h = \beta_D \omega_c$, which leads to $\xi_{ch} = \xi_{hc} = 1$ as it should.

III. GENERAL EXPRESSIONS FOR PERFORMANCE PARAMETERS

For the Otto cycle, the work is produced only in the two adiabatic branches, with heat produced along the isochoric processes. Initially, the time is assumed to be $t = 0$. The system Hamiltonian changes from $\hat{H}(\tau_h)$ to $\hat{H}(\tau_h + \tau_{hc})$ along the adiabatic expansion $B \rightarrow C$, and it goes back to $\hat{H}(0)$ from $\hat{H}(\tau_{cyc} - \tau_{ch})$ after the adiabatic compression $D \rightarrow A$. The system Hamiltonian is kept constant along each isochoric stroke, namely, $\hat{H}(0) = \hat{H}(\tau_h)$ and $\hat{H}(\tau_h + \tau_{hc}) = \hat{H}(\tau_{cyc} - \tau_{ch})$. The stochastic work done by the system per cycle is thus the total work output along the two adiabatic trajectories [30, 47], which reads $w[\hat{H}(\tau_h)|n]; \hat{H}(\tau_{cyc} - \tau_{ch})|m] = [\langle n|\hat{H}(\tau_h)|n\rangle - \langle n|\hat{H}(\tau_h + \tau_{hc})|n\rangle] + [\langle m|\hat{H}(\tau_{cyc} - \tau_{ch})|m\rangle - \langle m|\hat{H}(0)|m\rangle]$. Using $\varepsilon_k^h = \langle k|\hat{H}(0)|k\rangle = \langle k|\hat{H}(\tau_h)|k\rangle$, $\varepsilon_k^c = \langle k|\hat{H}(\tau_h + \tau_{hc})|k\rangle = \langle k|\hat{H}(\tau_{cyc} - \tau_{ch})|k\rangle$, with

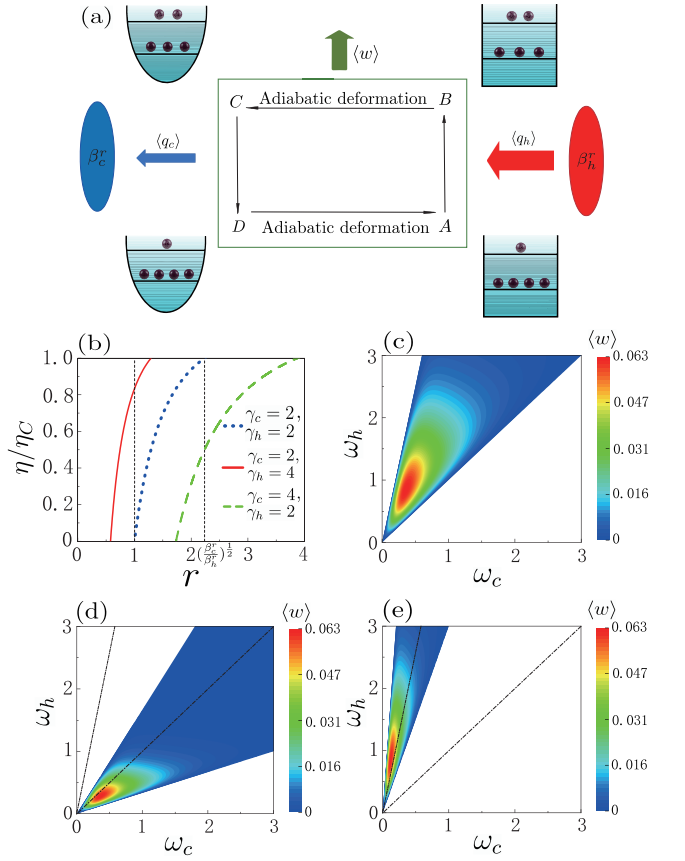


FIG. 1: (a) Sketch of the two-level Otto cycle. (b) Efficiency in unit of η_C versus ratio $r (= \sqrt{\omega_h/\omega_c})$ for different values of $\gamma_{c,h}$. The frequency is $\omega_c = 0.36$ in (c). The contour maps of $\langle w \rangle$ about ω_c and ω_h in the three cases ($\gamma_c = \gamma_h = 2$, $2\gamma_c = \gamma_h = 4$ and $\gamma_c = 2\gamma_h = 4$) are respectively drawn as (c), (d) and (e). The other parameters are $\beta_c^r = 10$ and $\beta_h^r = 2$ in (b), (c), (d) and (e).

$k = m, n$, we then arrive at

$$w[|n(\tau_h)\rangle; |m(\tau_{cyc} - \tau_{ch})\rangle] = \varepsilon_n^h - \varepsilon_n^c + \varepsilon_m^c - \varepsilon_m^h. \quad (3)$$

During the adiabatic stroke the level populations do not change, $p_{n,B} = p_{n,C}$ and $p_{m,A} = p_{m,D}$, the probability density of the stochastic work w then determined according to

$$p(w) = \sum_{n,m} p_{n,B} p_{m,A} \delta\{w - w[|n(\tau_h)\rangle; |m(\tau_{cyc} - \tau_{ch})\rangle]\}, \quad (4)$$

where $\delta(\cdot)$ is the Dirac's δ function. The average work output per cycle $\langle w \rangle = \int w p(w) dw$, can be obtained as $\langle w \rangle = \langle \hat{H}(\tau_h) \rangle - \langle \hat{H}(\tau_h + \tau_{hc}) \rangle + \langle \hat{H}(\tau_{cyc} - \tau_{ch}) \rangle - \langle \hat{H}(0) \rangle$, or $\langle w \rangle = \omega_h(g_B - g_A) + \omega_c(g_D - g_C)$ which, together with Eq. (2), gives rise to

$$\langle w \rangle = \left(\omega_h - \omega_c \frac{\xi_{hc} g_B - g_D}{g_B - \xi_{ch} g_D} \right) (g_B - \xi_{ch} g_D). \quad (5)$$

The work fluctuations can be determined according to

$$\langle \delta^2 w \rangle = \langle w^2 \rangle - \langle w \rangle^2, \quad (6)$$

where $\langle w^2 \rangle = \int w^2 p(w) dw = \sum_{n,m} p_{n,B} p_{m,A} (\varepsilon_n^h - \varepsilon_n^c + \varepsilon_m^c - \varepsilon_m^h)^2$.

Using the two-time measurement approach, the probability density function of the stochastic heat q_h along the hot isochoric stroke where no work is produced can be determined by the conditional probability to arrive at

$$p(q_h) = \sum_{n,m} p_{m \rightarrow n}^{\tau_h} p_{m,A} \delta[q_h - (\varepsilon_n^h - \varepsilon_m^h)], \quad (7)$$

where $p_{m,A}$ is the probability that the system is initially in state m at time $t = 0$, and $p_{m \rightarrow n}^{\tau_h}$ is the probability of the system collapsing into another state n after a time period τ_h . Here $p_{m \rightarrow n}^{\tau_h} |_{\tau_h \rightarrow \infty} = p_n^{eq}(\beta_h^r)$, where $p_n^{eq}(\beta_h^r) = e^{-\beta_h^r \varepsilon_n^h} / Z_h$ with $Z_h = \sum_n e^{-\beta_h^r \varepsilon_n^h}$. For each cycle, heat is transferred only in the isochore, while work is produced only along the adiabatic process. The heat absorbed from the hot squeezed bath is given by $\langle q_h \rangle = \langle \hat{H}(\tau_h) \rangle - \langle \hat{H}(0) \rangle$, or

$$\langle q_h \rangle = \omega_h (g_B - \xi_{ch} g_D). \quad (8)$$

In order to evaluate the average values of heat and work in a finite time cycle, we analyze the system dynamics along two isochoric strokes (see appendix A for details) to derive the expressions of these quantities (5) and (8) as

$$\begin{aligned} \langle w \rangle &= \left(\frac{1 - \xi_{hc} \xi_{ch} y}{1 - y} \omega_h - \xi_{hc} \omega_c \right) \\ &\times \left(g_h^{eq} - \frac{\xi_{ch} \omega_h - \frac{1 - \xi_{hc} \xi_{ch} x}{1 - x} \omega_c}{1 - \xi_{hc} \xi_{ch} y} g_c^{eq} \right) \mathcal{G}, \quad (9) \end{aligned}$$

and

$$\langle q_h \rangle = \omega_h \left(\frac{1 - \xi_{hc} \xi_{ch} y}{1 - y} g_h^{eq} - \xi_{ch} g_c^{eq} \right) \mathcal{G}, \quad (10)$$

where $\mathcal{G} = \frac{(1-x)(1-y)}{(1-\xi_{hc}\xi_{ch}xy)}$, with $x = e^{-\Sigma_h \tau_h}$ and $y = e^{-\Sigma_c \tau_c}$. The heat quantity released into the cold bath can be directly calculated by $\langle q_c \rangle = \langle w \rangle - \langle q_h \rangle$ due to the conservation of energy. Here Σ_c (Σ_h) denotes the thermal conductivity between the system and cold (hot) heat reservoir. The efficiency, $\eta = \langle w \rangle / \langle q_h \rangle$, then follows as

$$\eta = 1 - \frac{\omega_c \xi_{hc} g_h^{eq} - \frac{1 - \xi_{hc} \xi_{ch} x}{1 - x} g_c^{eq}}{\omega_h \frac{1 - \xi_{hc} \xi_{ch} y}{1 - y} g_h^{eq} - \xi_{ch} g_c^{eq}}, \quad (11)$$

which simplifies to $\eta = 1 - \frac{\omega_c \xi_{hc} g_h^{eq} - g_c^{eq}}{\omega_h g_h^{eq} - \xi_{ch} g_c^{eq}}$ in the quasi-static limit where $\tau_c \rightarrow \infty$ and $\tau_h \rightarrow \infty$. In case the shape of the potential is adiabatically changed, an inhomogeneous shift of energy levels is created, resulting in the thermodynamic efficiency (11) that depends on the shapes of the potentials along two isochoric strokes, except if these two potentials are identical to each other, making the efficiency reduce to the one for cycles without adiabatic shape deformation, $\eta = 1 - \omega_c / \omega_h$.

IV. PERFORMANCE AND STABILITY OF A TWO-LEVEL MACHINE

The efficiency may be enhanced by adiabatically changing the form of potential. To better understand the influence induced by adiabatic deformation on the performance of thermal machine, we investigate how the adiabatic deformation affects the efficiency and the power. In this section, we consider, as an example, the Otto engine working in the low-temperature limit, by assuming that only the two lowest energy levels are appreciably populated. As we show in Appendix B, the specific forms of g_B and g_D are

$$\begin{aligned} g_B &= g_h^{eq} + \left(\frac{\gamma_c - \gamma_h}{\gamma_c - 1} + \frac{\gamma_h - 1}{\gamma_c - 1} g_c^{eq} - g_h^{eq} \right) \frac{(1-y)x}{1-xy}, \\ g_D &= g_c^{eq} + \left(\frac{\gamma_h - \gamma_c}{\gamma_h - 1} + \frac{\gamma_c - 1}{\gamma_h - 1} g_h^{eq} - g_c^{eq} \right) \frac{(1-x)y}{1-xy}, \quad (12) \end{aligned}$$

where $g_c^{eq} = \frac{e^{-\beta_c^r \omega_c} + \gamma_c e^{-\gamma_c \beta_c^r \omega_c}}{e^{-\beta_c^r \omega_c} + e^{-\gamma_c \beta_c^r \omega_c}}$, and $g_h^{eq} = \frac{e^{-\beta_h^r \omega_h} + \gamma_h e^{-\gamma_h \beta_h^r \omega_h}}{e^{-\beta_h^r \omega_h} + e^{-\gamma_h \beta_h^r \omega_h}}$. The average work (9) and thermodynamic efficiency (11) of the two-level machine in finite time reduce to

$$\begin{aligned} \langle w \rangle &= \left(g_h^{eq} - \frac{\gamma_h - 1}{\gamma_c - 1} g_c^{eq} + \frac{\gamma_h - \gamma_c}{\gamma_c - 1} \right) \\ &\times \left(\omega_h - \frac{\gamma_c - 1}{\gamma_h - 1} \omega_c \right) \mathcal{G}, \quad (13) \end{aligned}$$

and

$$\eta = 1 - \frac{\omega_c}{\omega_h} \frac{\gamma_c - 1}{\gamma_h - 1}, \quad (14)$$

where $\gamma_c = 2^{\theta_c}$ and $\gamma_h = 2^{\theta_h}$ have been used. In such a case the work fluctuation $\langle \delta^2 w \rangle$ simplifies to

$$\begin{aligned} \langle \delta^2 w \rangle &= \langle w^2 \rangle - \langle w \rangle^2 \\ &= \frac{\gamma_h - 1}{\gamma_c - 1} \left[\omega_h - \omega_c \frac{\gamma_c - 1}{\gamma_h - 1} \right]^2 \\ &\times [(g_B - 1)(\gamma_c - g_D) + (g_D - 1)(\gamma_h - g_B)] \\ &- \left\{ \frac{1}{\gamma_c - 1} \left[\omega_h - \omega_c \frac{\gamma_c - 1}{\gamma_h - 1} \right] \right\}^2 \\ &\times [(g_B - 1)\gamma_c - (g_D - 1)\gamma_h + (g_D - g_B)]^2. \quad (15) \end{aligned}$$

The system reaches thermal equilibrium at the end of the hot or cold isochore when the process is quasi-static limit. In this case where $x \rightarrow 0$, $y \rightarrow 0$, and $\mathcal{G} = \frac{(1-x)(1-y)}{1-xy} \rightarrow 1$, the work (13) and work fluctuations (15) turn out to be

$$\begin{aligned} \langle w \rangle &= \left(g_h^{eq} - \frac{\gamma_h - 1}{\gamma_c - 1} g_c^{eq} + \frac{\gamma_h - \gamma_c}{\gamma_c - 1} \right) \\ &\times \left(\omega_h - \frac{\gamma_c - 1}{\gamma_h - 1} \omega_c \right), \quad (16) \end{aligned}$$

$$\begin{aligned}
\langle \delta^2 w \rangle &= \frac{\gamma_h - 1}{\gamma_c - 1} \left(\omega_h - \omega_c \frac{\gamma_c - 1}{\gamma_h - 1} \right)^2 \\
&\times [(g_h^{eq} - 1)(\gamma_c - g_c^{eq}) + (g_c^{eq} - 1)(\gamma_h - g_h^{eq})] \\
&- \left\{ \frac{1}{\gamma_c - 1} \left(\omega_h - \omega_c \frac{\gamma_c - 1}{\gamma_h - 1} \right) \right\}^2 \\
&\times [(g_h^{eq} - 1)\gamma_c - (g_c^{eq} - 1)\gamma_h + (g_c^{eq} - g_h^{eq})]^2.
\end{aligned} \tag{17}$$

In Fig. 1(b) we plot the normalized efficiency η/η_C at the quasi-static limit as a function of the ratio r (with $r \equiv \sqrt{\omega_h/\omega_c}$) in presence of adiabatic shape deformation, comparing corresponding result for the Otto engine without deformation of trap. In the absence of adiabatic deformation of trap ($\gamma_c = \gamma_h$), the three different conditions of the compression ratio r correspond to the three modes of the machine: (1) for $r \leq 1$ the machine operates as a heater, (2) for $1 < r \leq r_C \equiv \sqrt{\beta_c^r/\beta_h^r}$ it works as a heat engine, and (3) for $r > r_C$ it becomes a refrigerator. However, when adiabatically changing the shape of trapping potential, the machine can operate as a heat engine even in the boundaries (1) and (3). Figures 1(c), 1(d) and 1(e) show contour plots of the average work $\langle w \rangle$ versus ω_h and ω_c for different values of $\gamma_{c,h}$. The color areas indicate the positive work of the thermal machine as a heat engine, showing that the positive work condition is changed due to adiabatic deformation of trapping potential.

If the thermalization is complete along each isochore, the work fluctuations (17) as a function of the compression ratio r , both for $\gamma_c \leq \gamma_h$ and for $\gamma_c > \gamma_h$, are plotted in Fig. 2(a), where $\gamma_c = \gamma_h = 2, 2\gamma_c = \gamma_h = 4$, and $\gamma_c = 2\gamma_h = 4$. In contrast to the efficiency which is improved by increasing r for given γ_c and γ_h [Fig. 1(b)], the curves of average work $\langle w \rangle$ and work fluctuations $\langle \delta w^2 \rangle$ as a function of r may be parabolic-like [See Fig. 2(a)]. It can be observed from Fig. 2(a) that, while for $\gamma_c \leq \gamma_h$ the curves of work fluctuations and average work as functions r are linear, but they become parabolic when $\gamma_c > \gamma_h$. Both the work fluctuations $\langle \delta^2 w \rangle$ and average work $\langle w \rangle$ for $\gamma_c > \gamma_h$ are much smaller than corresponding those obtained from the case when $\gamma_c \leq \gamma_h$. The relative fluctuations, $\sqrt{\langle \delta^2 w \rangle} / \langle w \rangle$, which are not plotted in figures, are found to be monotonically increasing as r increases. As shown in Fig. 2(b), for given γ_c , improving efficiency by controlling γ_h would result in increasing relative power fluctuations $f_P = \sqrt{\langle \delta^2 w \rangle} / \langle w \rangle$ which, equivalent to the relative work fluctuations, can be used to describe the engine stability [17]. Figure 2(b) illustrates possible optimal realizations of the quantum heat engine with $\gamma_c \geq \gamma_h$. For example, operated at the efficiency $\eta = 0.7$, the engine with $\gamma_c = 2$ and $\gamma_h = 1.78$ ($\gamma_c = 4$ and $\gamma_h = 3.35$) works under the relative power fluctuations $f_P = 5.81$ ($f_P = 9.15$). It indicates that the quantum device can be optimally designed to increase stability by decreasing relative fluctuations f_P without sacrificing the thermodynamic efficiency η . Moreover, we observe that, $\eta = 0.74$ (> 0.7) and $f_P = 8.69$ (< 9.15) if $\gamma_c = 2$

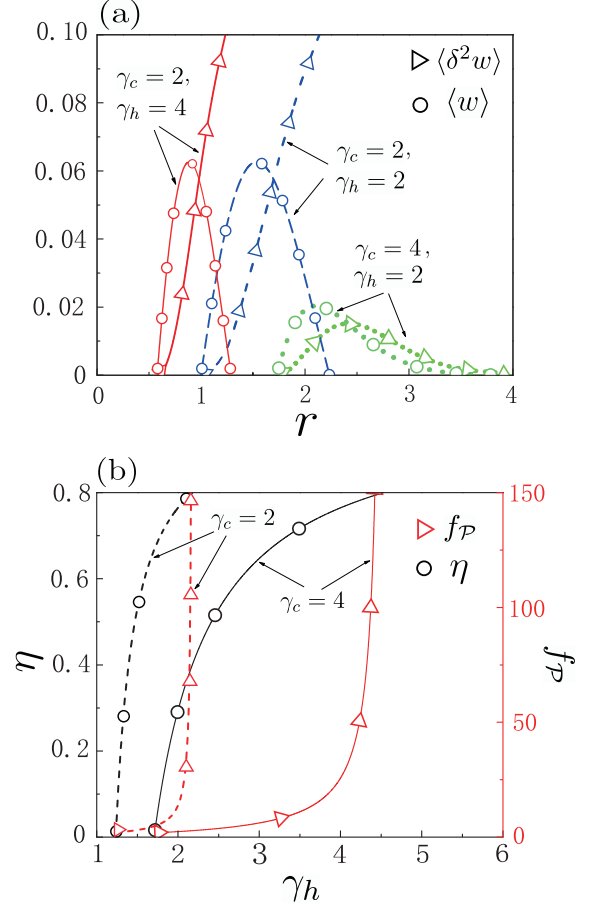


FIG. 2: Under quasi-static conditions, work fluctuations $\langle \delta^2 w \rangle$ and $\langle \delta w \rangle$ versus ratio $r (= \sqrt{\omega_h/\omega_c})$ for different values of $\gamma_{c,h}$ in (a). The efficiency and relative power fluctuation $f_P = \sqrt{\langle \delta^2 w \rangle} / \langle w \rangle$ versus γ_h are plotted in (b), where the parameters are set to $\omega_c = 0.2$ and $\omega_h = 0.85$. The other parameters are $\beta_c^r = 10$ and $\beta_h^r = 2$ in all cases

and $\gamma_h = 1.9$. If the forms of the potential are selected appropriately, the engine can run efficiently with high stability.

V. THE ENGINE UNDER MAXIMAL POWER OUTPUT

Since the power output, $\mathcal{P} = \langle w \rangle / \tau_{cyc}$, would vanish if the cycle is quasistatic and the cycle period, $\tau_{cyc} = \tau_h + \tau_c + \tau_{hc} + \tau_{ch}$, approaches infinity, piratically the engine should operate in finite time to produce finite power output. In this section we will consider the efficiency and power statistics for the two-level machine under maximum power by optimizing power with respect to external degrees. It is not difficult to verify that the efficiency at maximum power η^* can be determined by using the method shown in Appendix B to analytically obtain [11] $\eta_{anal}^* = \eta_C^2 / [\eta_C - (1 - \eta_C) \ln(1 - \eta_C)] = \eta_C / 2 + \eta_C^2 / 8 +$

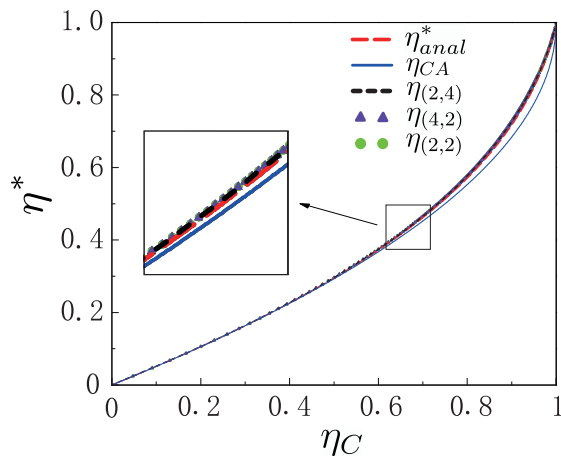


FIG. 3: Plots of analytical expression η_{anal}^* and exact numerical calculations for efficiency at maximum power, and plot of the CA efficiency η_{CA} . We use $\eta_{(\gamma_c, \gamma_h)}$ to denote these exact values of optimal efficiency for given γ_c and γ_h . The inverse temperature of hot bath is $\beta_h^r = 2$.

$O(\eta_C^3)$, which share the same universality with the CA efficiency [1, 3, 41] $\eta_{CA} = \eta_C/2 + \eta_C^2/8 + O(\eta_C^3)$.

In Fig. 3 we plot the analytical efficiency of maximum power η_{anal}^* as a function of the η_C , comparing the exact numerical result for different values of $\gamma_{c,h}$ and the CA efficiency η_{CA} . These curves of the optimal efficiency for different $\gamma_{c,h}$, together with the analytical expression of η_{anal}^* , collapse into a single line, and they are in nice agreement with the CA efficiency η_{CA} . It is therefore shown that, the efficiency at maximum power, agreeing well with η_{CA} , is independent of the shapes of the two trapping potentials. As emphasized, the heat can operate (as heat engine) under maximal power in regions beyond the engine in absence of adiabatic deformation and its classical counterpart.

VI. CONCLUSIONS

In summary, we have investigated the performance of quantum Otto engines in presence of potential deformation. With this deformation, the machine stability can be enhanced by decreasing relative power fluctuations, without sacrifice of the machine efficiency. When tuning the trap frequency, the efficiency at maximum power, independent of the shape deformation, shares the same universality with the CA efficiency. This optimal efficiency, however, can be realized in the regions where the classical can not operate as a heat engine. The shape deformation is vanishing the classical limit where the principle of the equipartition of energy holds, and it is therefore of purely quantum origin.

Appendix A: Time evolution for the system along an isochoric process

The quantum dynamics for a d -dimensional system is generated by external fields during the two adiabatic processes and by heat flows from hot and cold reservoirs in the two isochoric processes. During a system-bath interaction interval, the change in time of an operator \hat{X} can be described by the quantum master equation [11, 13],

$$\dot{\hat{X}} = i[\hat{H}, \hat{X}] + \frac{\partial \hat{X}}{\partial t} + \mathcal{L}_D(\hat{X}), \quad (\text{A.1})$$

where $\mathcal{L}_D(\hat{X}) = \sum_{\alpha} k_{\alpha} (\hat{V}_{\alpha}^{\dagger}[\hat{X}, \hat{V}_{\alpha}] + [\hat{V}_{\alpha}^{\dagger}, \hat{X}]\hat{V}_{\alpha})$ represents the Liouville dissipative generator, \hat{V}_{α} are operators in the Hilbert space of the system with their Hermitian conjugates $\hat{V}_{\alpha}^{\dagger}$, and k_{α} are phenomenological positive coefficients. Here and hereafter we use the dot to denote the differentiation with respect to time t . Substituting $\hat{H} = \hat{X}$ into Eq. (A.1), the first law of quantum thermodynamics is obtained as,

$$\dot{E} = \dot{W} + \dot{Q} = \left\langle \frac{\partial \hat{H}}{\partial t} \right\rangle + \langle \mathcal{L}_D(\hat{H}) \rangle, \quad (\text{A.2})$$

where $\dot{W} = \langle \partial \hat{H} / \partial t \rangle$ and $\dot{Q} = \langle \mathcal{L}_D(\hat{H}) \rangle$ are identified instantaneous power and heat flux, respectively. For a d -dimensional system under consideration, the operators \hat{V}^{\dagger} and \hat{V} , are chosen as the creation $\hat{a}_{\mathbf{i}}^{\dagger}$ and annihilation operator $\hat{a}_{\mathbf{i}}$, respectively, with $\mathbf{i} = \{i_1, i_2, \dots, i_d\}$ being nonnegative integers. By defining $\hat{H} = \sum_{\mathbf{i}} \varepsilon_{\mathbf{i}} \hat{a}_{\mathbf{i}}^{\dagger} \hat{a}_{\mathbf{i}}$ into Eq. (A.2), where $\mathcal{L}_D(\hat{X}) = \sum_{\mathbf{i}} \varepsilon_{\mathbf{i}} k_{\mathbf{i}}^u (\hat{a}_{\mathbf{i}}[\hat{X}, \hat{a}_{\mathbf{i}}^{\dagger}] + [\hat{a}_{\mathbf{i}}, \hat{X}]\hat{a}_{\mathbf{i}}^{\dagger}) + \varepsilon_{\mathbf{i}} k_{\mathbf{i}}^d (\hat{a}_{\mathbf{i}}^{\dagger}[\hat{X}, \hat{a}_{\mathbf{i}}] + [\hat{a}_{\mathbf{i}}^{\dagger}, \hat{X}]\hat{a}_{\mathbf{i}})$, we obtain the instantaneous population current as

$$\dot{Q} = -\Sigma(\langle \hat{H} \rangle - \langle \hat{H} \rangle^{eq}), \quad (\text{A.3})$$

where $\Sigma = k_{i_1, i_2, \dots, i_d}^d - k_{i_1, i_2, \dots, i_d}^u$ indicates the heat conductivity and $\langle \hat{H} \rangle^{eq} = \sum_{\mathbf{i}} \varepsilon_{\mathbf{i}} k_{\mathbf{i}}^u / (k_{\mathbf{i}}^d - k_{\mathbf{i}}^u)$ is the asymptotic value of $\langle \hat{H} \rangle$ at thermal equilibrium, with $k_{\mathbf{i}}^u / k_{\mathbf{i}}^d = \exp(-\beta \varepsilon_{\mathbf{i}})$ for a given trap.

Now we are in position to discuss the evolution of the system during system-bath interaction interval. For the finite-time process, the system assumed to be initially at time $t_A = 0$, evolves from the initial instant A to the final state B . On this branch heat is absorbed from the hot bath during a period τ_h while no work is done. The system would relax to the thermal state after infinite long time, and then $g_B|_{\tau_h \rightarrow \infty} = g_h^{eq} = g(\beta_h^r \omega_h, \sigma_h)$. From Eq. (A.3), we get

$$g_B = g_h^{eq} + (g_A - g_h^{eq}) e^{-\Sigma_h \tau_h}, \quad (\text{A.4})$$

where Σ_h is the heat conductivity between the working substance and the hot reservoir. For the cold isochore $C \rightarrow D$, the system is in contact with the cold reservoir at inverse temperature β_c in time of τ_c . Based on

an analogy with hot isochore $A \rightarrow B$, the dimensionless system energy g_D as a function g_C is obtained,

$$g_D = g_c^{eq} + (g_C - g_c^{eq})e^{-\Sigma_c \tau_c}, \quad (\text{A.5})$$

where $g_c^{eq} = g(\beta_c^r \omega_c, \sigma_c)$, and Σ_c represents the heat conductivity between the working substance and the cold reservoir. Having these formulae [(2), (A.4) and (A.5)], the relationship between $g(\tau_h)$ [$g(\tau_{cyc} - \tau_{ch})$] and its asymptotic value g_h^{eq} (g_c^{eq}) is easily obtained:

$$\begin{aligned} g_B &= g_h^{eq} - g_h^{eq} \frac{(1 - \xi_{hc} \xi_{ch} y)x}{1 - \xi_{hc} \xi_{ch} xy} + g_c^{eq} \frac{\xi_{ch}(1-y)x}{1 - \xi_{hc} \xi_{ch} xy}, \\ g_D &= g_c^{eq} - g_c^{eq} \frac{(1 - \xi_{hc} \xi_{ch} x)y}{1 - \xi_{hc} \xi_{ch} xy} + g_h^{eq} \frac{\xi_{hc}(1-x)y}{1 - \xi_{hc} \xi_{ch} xy}, \end{aligned} \quad (\text{A.6})$$

where we have used $x = e^{-\Sigma_h \tau_h}$ and $y = e^{-\Sigma_c \tau_c}$. As expected, when $\tau_h \rightarrow \infty$ ($\tau_{c,h} \rightarrow \infty$), $x, y \rightarrow 0$, $g_B|_{\tau_h \rightarrow \infty} \rightarrow g_h^{eq}$, $g_D|_{\tau_c \rightarrow \infty} \rightarrow g_c^{eq}$. Inserting Eq. (A.6) into Eqs. (5) and (8) in the main text leads to the time-dependent expressions of work and heat injection [Eqs. (9) and (10) in the main text].

Appendix B: Work (power) statistics for a two-level system

Without loss of generality, we consider one-dimensional power-law potentials whose single-particle energy spectrum takes the form

$$\varepsilon_n = \omega n^\theta, \quad (\text{B.1})$$

where $n = 1, 2, \dots$, and θ is a positive index depending on the form of the trapping potential. Several special case examples include [46]: (i) $\theta = 2$ for an infinite potential well, (ii) $\theta = 1$ for a harmonic potential, (iii) $\theta = 4/3$ for a quartic potential. When only the first two levels are populated for one-dimensional potential, the probabilities of these two levels at the end of the cold isochore are given by

$$p_{g,D} = \frac{e^{-\beta_D \omega_c}}{Z_D}, \quad p_{e,D} = \frac{e^{-\gamma_c \beta_D \omega_c}}{Z_D}, \quad (\text{B.2})$$

where $Z_D = e^{-\beta_D \omega_c} + e^{-\gamma_c \beta_D \omega_c}$ with $\gamma_c = 2^{\theta_c}$, and these two-level probabilities at the end of the hot isochore become

$$p_{g,B} = \frac{e^{-\beta_B \omega_h}}{Z_B}, \quad p_{e,B} = \frac{e^{-\gamma_h \beta_B \omega_h}}{Z_B}, \quad (\text{B.3})$$

where $Z_B = e^{-\beta_B \omega_h} + e^{-\gamma_h \beta_B \omega_h}$ with $\gamma_h = 2^{\theta_h}$. For example, when changing the harmonic trap in the cold isochore to the one-dimensional box trap, $\theta_c = 1$ and $\theta_h = 2$, but if the potential is one-dimensional box (harmonic) in the cold (hot) isochore, $\theta_c = 2$ and $\theta_h = 1$. In such a

case, the dimensionless energies ($g = \omega^{-1} \sum_n p_n \varepsilon_n$) at the special four instants [in Fig. 1(a)] can be written as

$$\begin{aligned} g_A &= \frac{1 + \gamma_h \chi_c}{1 + \chi_c}, \quad g_B = \frac{1 + \gamma_h \chi_h}{1 + \chi_h}, \\ g_C &= \frac{1 + \gamma_c \chi_h}{1 + \chi_h}, \quad g_D = \frac{1 + \gamma_c \chi_c}{1 + \chi_c}, \end{aligned} \quad (\text{B.4})$$

where we have used $\chi_c = e^{-(\gamma_c - 1)\beta_D \omega_c}$ and $\chi_h = e^{-(\gamma_h - 1)\beta_B \omega_h}$. Note that there is a relation:

$$\begin{aligned} g_A &= \frac{(\gamma_h - 1)g_D + \gamma_c - \gamma_h}{\gamma_c - 1}, \\ g_C &= \frac{(\gamma_c - 1)g_B + \gamma_h - \gamma_c}{\gamma_h - 1}. \end{aligned} \quad (\text{B.5})$$

When the times $\tau_{c,h} \rightarrow \infty$, the system reaches the thermal equilibrium at the end of either the hot or the cold isochore, indicating that $\beta_B \rightarrow \beta_h^r$ and $\beta_D \rightarrow \beta_c^r$. We therefore obtain g_h^{eq} and g_c^{eq} as $g_c^{eq} = \frac{e^{-\beta_c^r \omega_c} + \gamma_c e^{-\gamma_c \beta_c^r \omega_c}}{e^{-\beta_c^r \omega_c} + e^{-\gamma_c \beta_c^r \omega_c}}$, and $g_h^{eq} = \frac{e^{-\beta_h^r \omega_h} + \gamma_h e^{-\gamma_h \beta_h^r \omega_h}}{e^{-\beta_h^r \omega_h} + e^{-\gamma_h \beta_h^r \omega_h}}$ by using Eq. (B.4). Combining Eq. (B.5) with Eqs. (A.4) and (A.5), we then have Eq. (12) in the main text. With consideration of Eqs. (B.5), (12) and Eq. (2) in the main text, we get

$$\begin{aligned} \xi_{hc} &= \frac{\gamma_c - 1}{\gamma_h - 1} + \frac{\gamma_h - \gamma_c}{\gamma_h - 1} \\ &\times \frac{1}{\left[g_h^{eq} + \left(\frac{\gamma_c - \gamma_h}{\gamma_c - 1} + \frac{\gamma_h - 1}{\gamma_c - 1} g_c^{eq} - g_h^{eq} \right) \frac{(1-y)x}{1-xy} \right]}, \\ \xi_{ch} &= \frac{\gamma_h - 1}{\gamma_c - 1} + \frac{\gamma_c - \gamma_h}{\gamma_c - 1} \\ &\times \frac{1}{\left[g_c^{eq} + \left(\frac{\gamma_h - \gamma_c}{\gamma_h - 1} + \frac{\gamma_c - 1}{\gamma_h - 1} g_h^{eq} - g_c^{eq} \right) \frac{(1-x)y}{1-xy} \right]}. \end{aligned} \quad (\text{B.6})$$

Inserting Eq. (B.6) into Eqs. (9) and (11), we can obtain the expressions of average work and efficiency [Eqs.(13) and (14) in the main text], as well as the power output

$$\begin{aligned} \mathcal{P} &= \frac{[-(\gamma_h - 1)\omega_h + (\gamma_c - 1)\omega_c]}{(e^{-\beta_h^r \omega_h} + e^{-\gamma_h \beta_h^r \omega_h})(e^{-\beta_c^r \omega_c} + e^{-\gamma_c \beta_c^r \omega_c})} \\ &\times \left(e^{-\beta_h^r \omega_h - \gamma_c \beta_c^r \omega_c} - e^{-\gamma_h \beta_h^r \omega_h - \beta_c^r \omega_c} \right) \mathcal{G}_{\tau_{cyc}}^{-1}, \end{aligned} \quad (\text{B.7})$$

with consideration of Eqs. (B.1), (B.2), and (B.3), the work fluctuations (6) in the main text can be analytically expressed as

$$\begin{aligned} \langle \delta^2 w \rangle &= \langle w^2 \rangle - \langle w \rangle^2 \\ &= \frac{(\chi_c + \chi_h)[\omega_c(\gamma_c - 1) - (\gamma_h - 1)\omega_h]^2}{(\chi_c + 1)(\chi_h + 1)} \\ &\quad - \left[\frac{(\chi_c - \chi_h)[\omega_c(\gamma_c - 1) - (\gamma_h - 1)\omega_h]}{(\chi_c + 1)(\chi_h + 1)} \right]^2. \end{aligned} \quad (\text{B.8})$$

This, together with Eq.(B.4), gives rise to Eq. (15) in the main text. We are in a position to calculate the efficiency for the machine under maximal power. Since the power is a complicated function of the time-dependent protocols of the hot and cold strokes, we perform the optimization in the two steps. The first step is to maximize power with respect to times τ_c and τ_h by fixing ω_c and ω_h . We use τ_{adi} by defining $\tau_{adi} \equiv \tau_{hc} + \tau_{ch}$ to denote the total time spent on the two adiabatic strokes. In this step, by setting $\partial\mathcal{P}/\partial\tau_c = \partial(\mathcal{G}\tau_{cyc}^{-1})/\partial\tau_c = 0$ and $\partial\mathcal{P}/\partial\tau_h = \partial(\mathcal{G}\tau_{cyc}^{-1})/\partial\tau_h = 0$ we reproduce the optimal relation: $\Sigma_h[\cosh(\Sigma_c\tau_c) - 1] = \Sigma_c[\cosh(\Sigma_h\tau_h) - 1]$. Second, we maximize the power by tuning the external control parameters ω_c and ω_h (or γ_c and γ_h). Using $\partial\mathcal{P}/\partial\omega_c = \partial\mathcal{P}/\partial\omega_h = 0$ (or $\partial\mathcal{P}/\partial\gamma_c = \partial\mathcal{P}/\partial\gamma_h = 0$), we get

$$\frac{\chi'_c\beta_c^r[\omega_c(\gamma_c - 1) - \omega_h(\gamma_h - 1)]}{1 + \chi'_c} = \frac{\chi'_c - \chi'_h}{1 + \chi'_h}, \quad (\text{B.9})$$

$$\frac{\chi'_h\beta_h^r[\omega_c(\gamma_c - 1) - \omega_h(\gamma_h - 1)]}{1 + \chi'_h} = \frac{\chi'_c - \chi'_h}{1 + \chi'_c}, \quad (\text{B.10})$$

where $\chi'_c = e^{-\beta_c^r\omega_c(\gamma_c-1)}$ and $\chi'_h = e^{-\beta_h^r\omega_h(\gamma_h-1)}$. From Eqs.(B.9)and (B.10), we can derive $\sqrt{\frac{\chi'_h\beta_h^r}{\chi'_c\beta_c^r}} = \frac{1+\chi'_h}{1+\chi'_c}$ and $\frac{\omega_c(\gamma_c-1)}{\omega_h(\gamma_h-1)} = \frac{\beta_h^r \ln\chi'_c}{\beta_c^r \ln\chi'_h}$ to obtain $\omega_c(\gamma_c - 1) - \omega_h(\gamma_h - 1) = \frac{\chi'_c - \chi'_h}{\sqrt{\beta_c^r\beta_h^r\chi'_c\chi'_h}}$. With these, one can prove after simple algebra [23] that the efficiency at maximum power can be written in terms of the Carnot efficiency η_C : $\eta^* = \eta_C^2/[\eta_C - (1 - \eta_C)\ln(1 - \eta_C)]$.

Acknowledgements

This work is supported by Natural Science Foundation of China (Grants No. 11875034), and the Opening Project of Shanghai Key Laboratory of Special Artificial Microstructure Materials and Technology.

-
- [1] F. Curzon and B. Ahlborn, *Efficiency of a Carnot engine at maximum power output*, Am. J. Phys. **43**, 22 (1975).
[2] N. Shiraishi, K. Saito, and H. Tasaki, *Universal trade-off relation between power and efficiency for heat engines*, Phys. Rev. Lett. **117**, 190601 (2016).
[3] S. Q. Sheng and Z. C. Tu, *Weighted reciprocal of temperature, weighted thermal flux, and their applications in finite-time thermodynamics*, Phys. Rev. E **89**, 012129 (2014).
[4] C. Wu, L. Chen, and J. Chen, *Advances in Finite-Time Thermodynamics: Analysis and Optimization* (Nova Science, New York, 2004).
[5] J. Lin, K. Li, J. Z. He, J. Ren, and J. H. Wang, *Power statistics of Otto heat engines with the Mpemba effect*, Phys. Rev. E **105**, 014104 (2022).
[6] J. Gonzalez-Ayala, J. C. Guo, A. Medina, J. M. M. Roco, A. C. Hernández, *Energetic self-optimization induced by stability in low-dissipation heat engines*, Phys. Rev. Lett. **124**, 050603 (2020).
[7] P. Pietzonka and U. Seifert, *Universal trade-off between power, efficiency and constancy in steady-state heat engines*, Phys. Rev. Lett. **120**, 190602 (2018).
[8] K. Proesmans, B. Cleuren, and C. Van den Broeck, *Power-Efficiency-Dissipation Relations in Linear Thermodynamics*, Phys. Rev. Lett. **116**, 220601 (2016).
[9] O. Raz, Y. Subaşı, and R. Pugatch, *Geometric heat engines featuring power that grows with efficiency*, Phys. Rev. Lett. **116**, 160601 (2016).
[10] K. Brandner, K. Saito, and U. Seifert, *Thermodynamics of Micro- and Nano-Systems Driven by Periodic Temperature Variations*, Phys. Rev. X **5**, 031019 (2015).
[11] J. H. Wang, Z. L. Ye, Y. M. Lai, W. S. Li, and J. Z. He, *Efficiency at maximum power of a quantum heat engine based on two coupled oscillators*, Phys. Rev. E **91**, 062134 (2015).
[12] V. Mehta and R. S. Johal, *Quantum Otto engine with exchange coupling in the presence of level degeneracy*, Phys. Rev. E **96**, 032110 (2017).
[13] R. Kosloff and A. Levy, *Quantum heat engines and refrigerators: Continuous devices*, Annu. Rev. Phys. Chem. **65**, 365 (2014).
[14] M. O. Scully, *Quantum afterburner: Improving the efficiency of an ideal heat engine*, Phys. Rev. Lett. **88**, 050602 (2002).
[15] J. Y. Du, W. Shen, X. Zhang, S. H. Su, and J. C. Chen, *Quantum-dot heat engines with irreversible heat transfer*, Phys. Rev. Research. **2**, 013259 (2020).
[16] D. Z. Xu, C. Wang, Y. Zhao, and J. S. Cao, *Polaron effects on the performance of light-harvesting systems: a quantum heat engine perspective*, New J. Phys. **18**, 023003 (2016).
[17] Q. Bouton, J. Nettersheim, S. Burgardt, D. Adam, E. Lutz, and A. Widera, *A quantum heat engine driven by atomic collisions*, Nat. Commun. **12**, 2063 (2021).
[18] L. Q. Wang, Z. Wang, C. Wang, and J. Ren, *Cycle Flux Ranking of Network Analysis in Quantum Thermal Devices*, arXiv: 2107. 07717
[19] J. Rofinagel, O. Abah, F. Schmidt-Kaler, K. Singer, and E. Lutz, *Nanoscale heat engine beyond the carnot limit*, Phys. Rev. Lett. **112**, 030602 (2014).
[20] K. E. Dorfman, D. Z. Xu, and J. S. Cao, *Efficiency at maximum power of a laser quantum heat engine enhanced by noise-induced coherence*, Phys. Rev. E **97**, 042120 (2018).
[21] R. Uzdin, A. Levy, and R. Kosloff, *Equivalence of quantum heat machines, and quantum-thermodynamic signatures*, Phys. Rev. X **5**, 031044 (2015).
[22] J. Klaers, S. Faelt, A. Imamoglu, and E. Togan, *Squeezed thermal reservoirs as a resource for a nanomechanical engine beyond the carnot limit*, Phys. Rev. X **7**, 031044 (2017).
[23] J. H. Wang, J. Z. He, and Y. L. Ma, *Finite-time performance of a quantum heat engine with a squeezed thermal bath*, Phys. Rev. E **100**, 052126 (2019).

- [24] K. Zhang and W. Zhang, *Quantum optomechanical straight-twin engine*, Phys. Rev. A **95**, 053870 (2017).
- [25] W. Niedenzu, V. Mukherjee, A. Ghosh, A. G. Kofman, and G. Kurizki, *Quantum engine efficiency bound beyond the second law of thermodynamics*, Nat. Commun. **9**, 165 (2018).
- [26] V. Singh and Özgür E. Müstecaplıoğlu, *Performance bounds of nonadiabatic quantum harmonic Otto engine and refrigerator under a squeezed thermal reservoir*, Phys. Rev. E **102**, 062123 (2020).
- [27] S. H. Raja, S. Maniscalco, G. S. Paraoanu, J. P. Pekola, and N. L. Gullo, *Finite-time quantum Stirling heat engine*, New J. Phys. **23**, 033034 (2021).
- [28] M. Campisi, J. Pekola, and R. Fazio, *Nonequilibrium fluctuations in quantum heat engines: theory, example, and possible solid state experiments*, New J. Phys. **17**, 035012 (2015).
- [29] W. Niedenzu, D. Gelbwaser-Klimovsky, A. G. Kofman, and G. Kurizki, *On the operation of machines powered by quantum non-thermal baths*, New J. Phys. **18**, 083012 (2016).
- [30] G. Q. Jiao, S. B. Zhu, J. Z. He, Y. L. Ma, and J. H. Wang, *Fluctuations in irreversible quantum Otto engines*, Phys. Rev. E **103**, 032130 (2021).
- [31] T. Denzler and E. Lutz, *Efficiency fluctuations of a quantum heat engine*, Phys. Rev. Research. **2**, 032062 (2020)
- [32] G. Verley, T. Willaert, C. Van den Broeck, and M. Esposito, *Universal theory of efficiency fluctuations*, Phys. Rev. E **90**, 052145 (2014).
- [33] N. M. Myers, O. Abah, and S. Deffner, *Quantum thermodynamic devices: from theoretical proposals to experimental reality*, arXiv: 2201.01740.
- [34] R. J. de Assis, T. M. de Mendonça, C. J. Villas-Boas, A. M. de Souza, R. S. Sarthour, I. S. Oliveira, and N. G. de Almeida, *Efficiency of a Quantum Otto Heat Engine Operating under a Reservoir at Effective Negative Temperatures*, Phys. Rev. Lett. **122**, 240602 (2019).
- [35] J. P. S. Peterson, T. B. Batalhão, M. Herrera, A. M. Souza, R. S. Sarthour, I. S. Oliveira, and R. M. Serra, *Experimental Characterization of a Spin Quantum Heat Engine*, Phys. Rev. Lett. **123**, 240601 (2019).
- [36] G. Benenti, K. Saito, and G. Casati, *Thermodynamic Bounds on Efficiency for Systems with Broken Time-Reversal Symmetry*, Phys. Rev. Lett. **106**, 230602 (2011).
- [37] A. E. Allahverdyan, K. V. Hovhannisyanyan, A. V. Melkikh, and S. G. Gevorkian, *Carnot Cycle at Finite Power: Attainability of Maximal Efficiency*, Phys. Rev. Lett. **111**, 050601 (2013).
- [38] M. Polettini, G. Verley, and M. Esposito, *Efficiency Statistics at All Times: Carnot Limit at Finite Power*, Phys. Rev. Lett. **114**, 050601 (2015).
- [39] K. Proesmans and C. Van den Broeck, *Onsager Coefficients in Periodically Driven Systems*, Phys. Rev. Lett. **115**, 090601 (2015).
- [40] M. Campisi and R. Fazio, *The power of a critical heat engine*, Nat. Commun. **7**, 11895 (2016).
- [41] R. S. Johal, *Heat engines at optimal power: Low-dissipation versus endoreversible model*, Phys. Rev. E **96**, 012151 (2018).
- [42] T. Feldmann and R. Kosloff, *Quantum four-stroke heat engine: Thermodynamic observables in a model with intrinsic friction*, Phys. Rev. E **68**, 016101 (2003).
- [43] H. T. Quan, Y. X. Liu, C. Sun, and F. Nori, *Quantum thermodynamic cycles and quantum heat engines*, Phys. Rev. E **76**, 031105 (2007).
- [44] D. Gelbwaser-Klimovsky, A. Bylinskii, D. Gangloff, R. Islam, A. Aspuru-Guzik, and V. Vuletic, *Single-Atom Heat Machines Enabled by Energy Quantization*, Phys. Rev. Lett. **120**, 170601 (2018).
- [45] P. W. H. Pinkse, A. Mosk, M. Weidemüller, M. W. Reynolds, T. W. Hijmans, and J. T. M. Walraven, *Adiabatically Changing the Phase-Space Density of a Trapped Bose Gas*, Phys. Rev. Lett. **78**, 990 (1997).
- [46] J. H. Wang, J. Z. He, and X. He, *Performance analysis of a two-state quantum heat engine working with a single-mode radiation field in a cavity*, Phys. Rev. E **84**, 041127 (2011)
- [47] V. Holubec and A. Ryabov, *Cycling Tames Power Fluctuations near Optimum Efficiency*, Phys. Rev. Lett. **121**, 120601 (2018).